

KUMARS SEIFPANAHI SHABANI\*<sup>1</sup>, FARAMARZ DOULATI ARDEJANI\*, KHSHAYAR BADI\*\*,  
MOHAMMAD EBRAHIM OLYA\*\*

**ACID MINE DRAINAGE TREATMENT BY PERLITE NANOMINERAL,  
BATCH AND CONTINUOUS SYSTEMS**

**OCZYSZCZANIE KWAŚNYCH WÓD KOPALNIA NYCH PRZY WYKORZYSTANIU NANOMINER A LU  
PERLITU – SYSTEMY DZIAŁANIA CIĄGŁEGO I OKRESOWEGO**

In this paper the adsorption activity of perlite nanoparticles for removal of  $\text{Cu}^{2+}$ ,  $\text{Fe}^{2+}$  and  $\text{Mn}^{2+}$  ions at Iran Sarcheshmeh copper acid mine drainage was discussed. Thus, raw perlite that provided from internal resource was modified and prepared via particles size reduction to nano scale and characterized by X-ray diffraction, X-ray fluorescence, scanning electron microscopy, transmission electron microscopy, Fourier transforms infrared and BET specific surface area analysis. The results of acid mine drainage show that pH of acid mine drainage is 5.1 and  $\text{Cu}^{2+}$ ,  $\text{Fe}^{2+}$  and  $\text{Mn}^{2+}$  ions are 10.5, 4.1 and 8.3 ppm, respectively. Firstly in the batch system the influence of adsorbent dose and temperature parameters were considered and then isothermal and kinetic models were investigated. According to the results the Langmuir isotherm and pseudo-second order kinetic model showed better correlation with the experimental data than other isotherm and kinetic models. Obtained thermodynamic parameters such as  $\Delta G^\circ$ ,  $\Delta H^\circ$  and  $\Delta S^\circ$  show that the  $\text{Cu}^{2+}$ ,  $\text{Fe}^{2+}$  and  $\text{Mn}^{2+}$  ions adsorption from acid mine drainage is spontaneous and endothermic. Finally, perlite nanoparticles adsorbent was packed inside a glass column and used for the removal of heavy metals in 1, 3, 5 ml/min acid mine drainage flow rates, the breakthrough curves show that the column was saturated at 180, 240 and 315 min for different flow rates, respectively. According to the obtained results, this abundant, locally available and cheap silicate mineral showed a great efficiency for the removal of heavy metal pollutants from acid mine drainage and can be utilized for much volume of acid mine drainage or industrial scale.

**Keywords:** Acid mine drainage, Perlite nanoparticles,  $\text{Cu}^{2+}$ ,  $\text{Fe}^{2+}$  and  $\text{Mn}^{2+}$  ions adsorption, Sarcheshmeh porphyry copper mine, batch and continuous systems

W pracy omówiono zdolności adsorpcyjne nano-cząsteczek perlitu wykorzystywanych o usuwania jonów  $\text{Cu}^{2+}$ ,  $\text{Fe}^{2+}$  i  $\text{Mn}^{2+}$  z kwaśnych wód kopalniach w kopalni miedzi w Sarcheshmeh w Iranie. Surowy perlit pozyskiwany ze źródeł własnych został zmodyfikowany i odpowiednio spreparowany poprzez zre-

\* DEPARTMENT OF MINING ENGINEERING, FACULTY OF MINING, PETROLEUM AND GEOPHYSICS, SHAHROOD UNIVERSITY OF TECHNOLOGY, SHAHROOD, IRAN

\*\* DEPARTMENT OF ENVIRONMENT, INSTITUTE FOR COLOR SCIENCE AND TECHNOLOGY, TEHRAN, IRAN

<sup>1</sup> CORRESPONDING AUTHOR: E-mail: [q.s11063@yahoo.com](mailto:q.s11063@yahoo.com)

dukowanie cząsteczek do rozmiarów rzędu nano- cząsteczek. Perlit poddany został następnie badaniom z wykorzystaniem dyfrakcji promieniowania rentgenowskiego, rentgenowskiej analizy fluorescencyjnej, skaningowej mikroskopii elektronowej, transmisyjnej mikroskopii elektronowej, spektroskopii w podczerwieni z transformacją Fouriera. Przeprowadzono także badania powierzchni właściwej w oparciu o równanie BET. Wyniki badań kwaśnych wód kopalnianych wykazują ich kwasowość na poziomie 5.1, a zawartość jonów  $\text{Cu}^{2+}$ ,  $\text{Fe}^{2+}$  i  $\text{Mn}^{2+}$  wynosi odpowiednio 10.5, 4.1, 8.3 ppm. W pierwszym etapie analizowano system działania okresowego, zbadano wpływ następujących parametrów: ilości czynnika absorbującego i temperatury. Następnie przebadano modele izotermiczne i kinetyczne. Na podstawie uzyskanych wyników wykazano, że izoterma Langmuira oraz model pseudo-kinetycznego drugiego rzędu wykazują lepszą zgodność z danymi eksperymentalnymi niż pozostałe modele izotermiczne i kinetyczne. Uzyskane parametry termodynamiczne:  $\Delta G^\circ$ ,  $\Delta H^\circ$  i  $\Delta S^\circ$  wskazują, że adsorpcja jonów  $\text{Cu}^{2+}$ ,  $\text{Fe}^{2+}$  i  $\text{Mn}^{2+}$  z kwaśnych wód kopalnianych przebiega spontanicznie i jest procesem endotermicznym. W końcowym etapie badania nanocząsteczki perlitu- adsorbentu zostały umieszczone wewnątrz szklanej kolumny i wykorzystane do usuwania jonów metali ciężkich z kwaśnych wód kopalnianych podawanych z prędkością przepływu 1, 3, 5 ml/min. Krzywe przebiecia wskazują, że kolumna została nasycona odpowiednio po 180, 240 i 315 dla odpowiednich prędkości przepływu. Uzyskane wyniki wskazują, że ten występujący lokalnie w dużych ilościach, tani i łatwo dostępny minerał krzemianowy wykazuje wysoką skuteczność w usuwaniu z kwaśnych wód kopalniach zanieczyszczeń w postaci metali ciężkich, dlatego też może być z powodzeniem wykorzystany do oczyszczania znacznych ilości wód a także na skalę przemysłową.

**Słowa kluczowe:** nanocząsteczki perlitu, adsorpcja jonów  $\text{Cu}^{2+}$ ,  $\text{Fe}^{2+}$  i  $\text{Mn}^{2+}$ , kopalnia miedzi i porfirów Sarcheshmeh, systemy działania ciągłego i okresowego

## 1. Introduction

Contamination of water by heavy metals is a global problem (Danil de Namor et al., 2012), as, heavy metal ions consist of iron, lead, manganese, zinc, copper, chromium, nickel and cadmium and so on lead to many problems for human and air/soil/water environment. In the environment two main sources of heavy metals are natural background that derived from parent rocks and anthropogenic contamination including mineral industrial wastes, tailing dumps of sulfide mines, agrochemicals and other output of industrial activities and factories (Li et al., 2012). Several conventional methodologies such as precipitation (Martin et al., 2010), ion exchange (Yuan et al., 2010), filtration membrane technology (Song et al., 2011), electrochemical processes (Karami, 2013) and adsorption process (Chiban et al., 2011) are available for heavy metal removal and other pollutants from wastewaters. Generally, they are expensive or ineffective sometimes, especially when the metal concentration is higher than 100 ppm (Schiewer and Volesky, 1995; Miretzky et al., 2006). Among all the treatments proposed, adsorption process is a popular method. It is now recognized as an effective, efficient and economic method for water decontamination applications and for separation to pilot purpose (Niu et al., 2007). Nowadays, the adsorption of pollutants by natural materials has been widely reported such as diatomite (Caliskan et al., 2011), perlite (Ghassabzadeh et al., 2010), red mud (Lopez et al., 2012), chitosan (Kyzas et al., 2013), orange skin (Lugo et al., 2012), soy meal hull (Badii et al., 2008), almond skin (Doulati Ardejani et al., 2008), dead fungi biomass (Seifpanahi et al., 2011), sawdust (Pehlivan & Altun, 2008), zeolite (Egashira et al., 2012) and clay (Sheikhhosseini et al., 2013), these adsorbents have natural base and they are environmental friendly and it is possible to be regenerated most of them or be applied in different products, and also was used for synthetic wastewaters, usually. Acid mine drainage generation at Sarcheshmeh mine was happened and this acid drainage that caused many problems, was entered to surface and groundwater's. So, in this paper treatment of acid mine drainage consist of heavy metal ions by natural adsorbents with nanoscale particles size was

done. So, the objective of the present study is focused on the development perlite nanoparticles for removal of heavy metal ions consist of  $\text{Cu}^{2+}$ ,  $\text{Fe}^{2+}$  and  $\text{Mn}^{2+}$  ions from Sarcheshmeh porphyry copper acid mine drainage.

## 2. Materials and Methods

In this research the raw perlite samples were obtained from internal sources, Zanjan mine at North West of Iran (Fig. 1).



Fig. 1. Perlite reservoirs in the Zanjan mines (N-W of Iran) and Sarcheshmeh copper mine (S-E of Iran)

The Sarcheshmeh copper mine is located at the South East part of Iran (Fig. 1). In this mine the results of acid mine drainage chemical analysis that was entered to Shur River, were showed at Table 1.

TABLE 1

The results of acid mine drainage chemical analysis

Ion	$\text{Fe}^{2+}$	$\text{Mn}^{2+}$	$\text{Cu}^{2+}$	$\text{Al}^{3+}$	$\text{Mo}^{2+}$	$\text{Pb}^{2+}$	$\text{Ni}^{2+}$	$\text{Ag}^{2+}$
Concentration (ppm)	4.1	8.3	10.5	0.24	0.29	0.65	0.003	0.057
SDWR (USEPA, 2011)	0.3	0.05	1	0.05-0.2	0.04	0	0.01	0.1

According to Table 1 the  $\text{Cu}^{2+}$ ,  $\text{Fe}^{2+}$  and  $\text{Mn}^{2+}$  ions have very higher range than Secondary Drinking Water Regulation (SDWR) of United State Environmental Protection Agency (USEPA). So for removal of  $\text{Cu}^{2+}$ ,  $\text{Fe}^{2+}$  and  $\text{Mn}^{2+}$  ions from Sarcheshmeh acid mine drainage the perlite nanoadsorbent was used.

In assessing the potential applications of perlite as nano for the removal of heavy metal ions from acid mine drainage, the modification of the material is an important issue to address. A variety of methodologies can be used to modify the perlite surface such as calcinations (Ghassabzadeh et al., 2010; Ediz et al., 2010; Jing et al., 2011), functionalization (Thanh et al., 2011; Fowler et al., 2007). So, raw perlite five times was washed with deionized water and then dried at  $100^{\circ}\text{C}$  for 8h. Next the samples were crushed by laboratory planetary ball mill (Fritsch Pulverisette 6 model) consist of distilled water in 250 rpm for 5h. Finally, slurry samples were dehumidifying by spray dryer (B-290 model) in  $180^{\circ}\text{C}$  and prepared for investigation the adsorption processes of heavy metal ions and characterization.

The chemical composition of the modified perlite nanoparticles which were determined by XRF 1800 model is given in Table 2.

TABLE 2

The chemical analysis of modified perlite nanoparticles

Constituent	Modified perlite nanoparticles (wt. %)
$\text{SiO}_2$	56.87
$\text{K}_2\text{O}$	17.70
$\text{Al}_2\text{O}_3$	18.36
$\text{Na}_2\text{O}$	2.61
$\text{Fe}_2\text{O}_3$	2.53
$\text{CaO}$	0.96
$\text{ZrO}_2$	0.19
$\text{MgO}$	0.20
$\text{SO}_3$	0.27
$\text{TiO}_2$	0.17
$\text{MnO}_2$	0.13

According to Table 2, modified perlite nanoparticles are mainly composed of silica as  $\text{SiO}_2$ . The hydroxyl species on perlite structure were identified as a function for adsorption process. Thus various hydroxyl species including isolated hydroxyl groups, H-bonded hydroxyl groups and water uptake have been identified for perlite (Yuan et al., 2004). Generally, the hydroxyl groups are classified according to their coordination to the silicon atom that was showed as Fig. 2.

The BET specific surface area analysis Quantachrome 2200e model was done for modified perlite nanoparticles and raw perlite is show in Table 3.

TABLE 3

BET Specific surface area of modified perlite nanoparticles and raw unmodified perlite

Material	Specific surface area ( $\text{m}^2/\text{gr}$ )
Modified perlite nanoparticles	89.7
Raw perlite	3.5

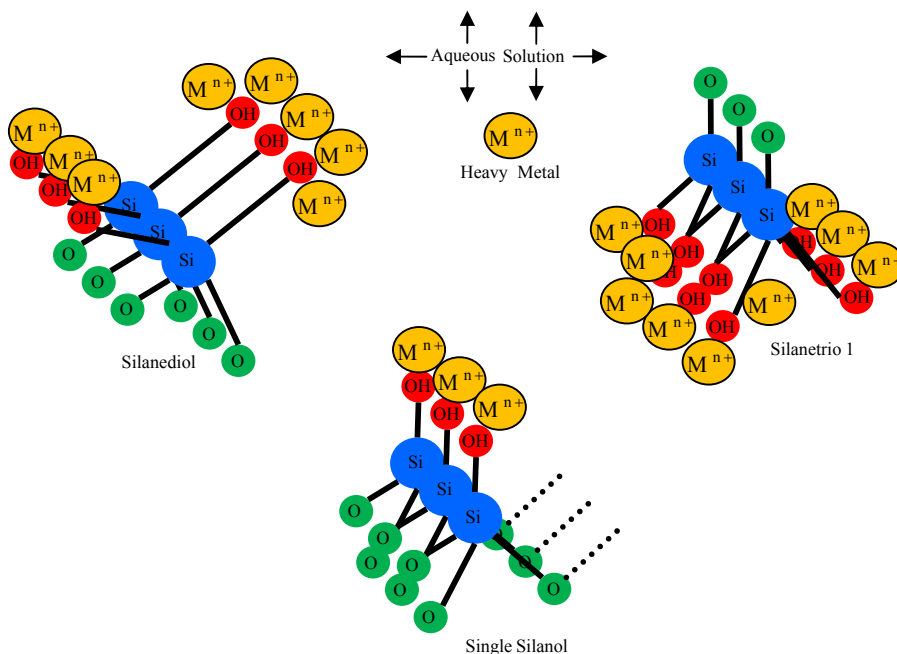


Fig. 2. The various arrays of hydroxyl groups that show for SiO<sub>2</sub> (Danil de Namor et al., 2012)

According to Muller (2010) researches the increase in surface area by decreasing the particle size of the perlite resulted in a higher uptake of heavy metal ions by the smaller particles relative to the larger ones (Muller, 2010).

The X-ray diffraction (XRD) patterns for modified perlite nanoparticles were obtained by XMD300-Unisantis X-ray diffractometer is show in Fig. 3.

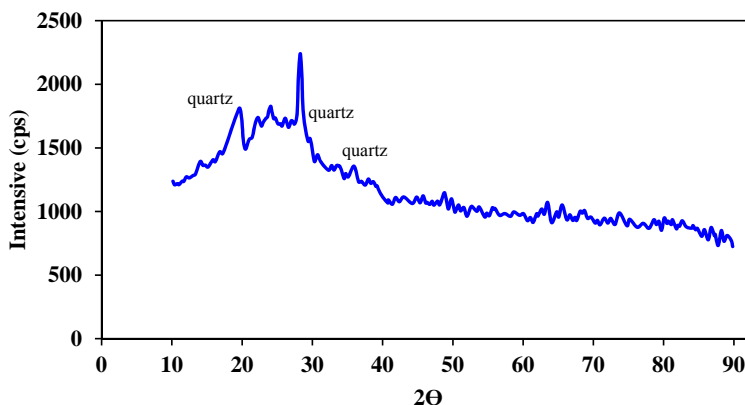


Fig. 3. XRD pattern of modified perlite nanoparticles

Scanning electron microscopy (SEM) LEO-1455VP model and the transmission electron microscope (TEM) PHILIPS CM120 model were used to study the morphology and homogeneity of the modified perlite nanoparticles.

The SEM (Fig. 4A) and TEM (Fig. 4B) images show the pure modified perlite nanoparticles. Generally, Fig. 4 shows the modified perlite nanoparticles that has an amorphous (Fig. 4A) granular (Fig. 4B) morphology with an average diameter of 150-200 nm.

The FT-IR technique is one of the most important characterization techniques used to elucidate the changes in chemical structures. FT-IR spectra of modified perlite nanoparticles for 1 min are shown in Fig. 5.

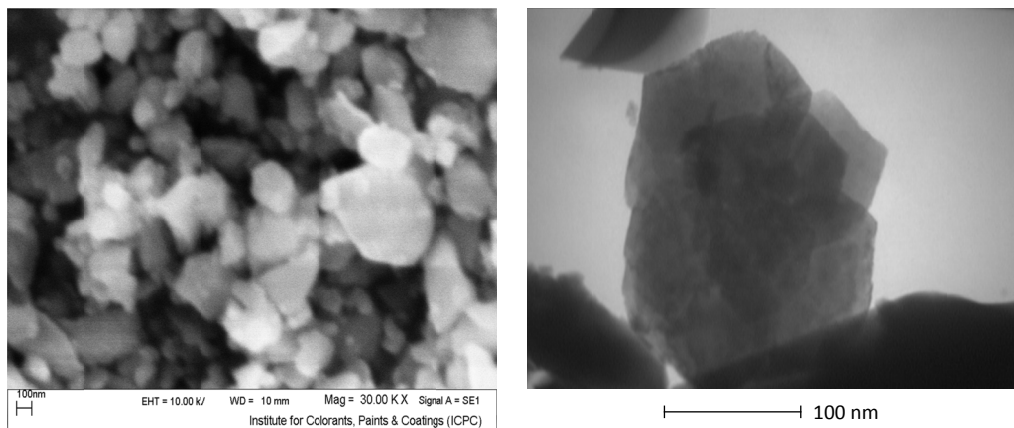


Fig. 4. SEM (A) and TEM (B) images for modified perlite nanoparticles

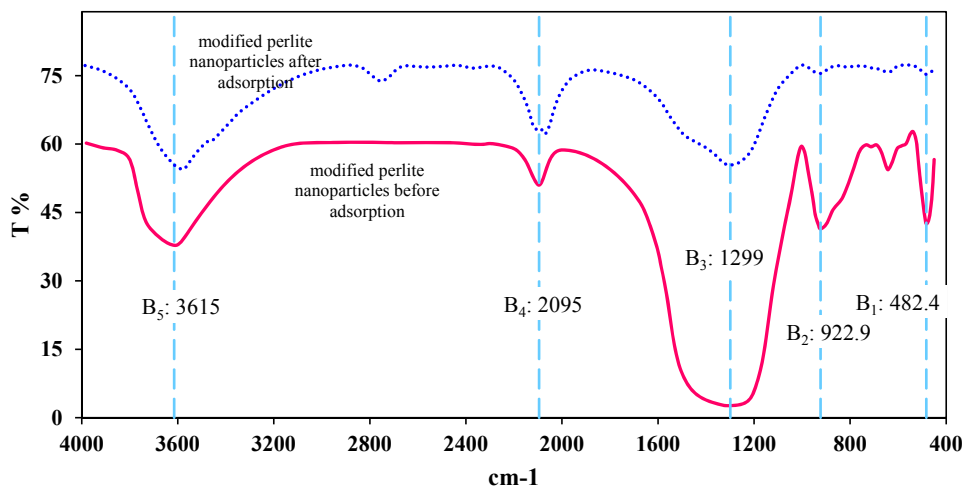


Fig. 5. FT-IR spectrum of the modified perlite nanoparticles before (————) and after (.....) ions adsorption process from acid mine drainage

According to Fig. 5, modified perlite nanoparticles five main absorption bands are observed at  $482.4\text{ cm}^{-1}$  ( $B_1$ ),  $922.9\text{ cm}^{-1}$  ( $B_2$ ),  $1299\text{ cm}^{-1}$  ( $B_3$ ),  $2095\text{ cm}^{-1}$  ( $B_4$ ) and  $3615\text{ cm}^{-1}$  ( $B_5$ ). Bands  $B_1$  and  $B_2$  are attributed to the Si–O stretching vibrations of Si–O–Si and Si–O–Al, respectively (Sodeyama et al., 1999). Band  $B_3$  is the deformation band of molecular water (Rouliia et al., 2006; Varuzhanyan et al., 2006). Band  $B_4$  is attributed to molecular adsorbed water (Sodeyama et al., 1999). Band  $B_5$  is attributed to the combination of OH stretching arising from hydrogen-bonded and free Si–OH (Hong and Minoru, 1994; Sodeyama et al., 1999). The intensities of bands  $B_3$ ,  $B_4$  and  $B_5$  are closely related to the water content, similar to other silicate materials and minerals, such as volcanic tuffs and zeolites. Development of the silicate network has been attributed to de-hydroxylation of mainly Si–OH (see Fig. 2) groups during any thermal and chemical treatment, including those treatments that do not lead to modification (Rouliia et al., 2006). On the other hand in Fig. 5, the FT-IR spectra of modified perlite nanoparticles before and after ions adsorption from acid mine drainage was showed. As is obvious the band  $B_5$  was OH weaken after ions adsorption from acid mine drainage than before adsorption that due to OH function saturating by  $\text{Cu}^{2+}$ ,  $\text{Fe}^{2+}$  and  $\text{Mn}^{2+}$  ions and so on.

## 2. Environmental application

### 2.1. Batch mode adsorption studies

Acid mine drainage solutions were prepared from Sarcheshmeh copper porphyry mine and followed by batch adsorption studies at  $25^\circ\text{C}$  on a multi stirrer hot plate to investigate the sorption processes. Known mass of modified perlite nanoparticles was added to a 25 mL of acid mine drainage solution, thoroughly mixed, and allowing sufficient time for equilibrium. Fast filtration followed and remaining metal ion concentrations were determined directly in the supernatant solution by flame atomic absorption spectrometry PG-990 model. The percentage adsorption of  $\text{Cu}^{2+}$ ,  $\text{Fe}^{2+}$  and  $\text{Mn}^{2+}$  heavy metals from aqueous solution was computed as follows:

$$\text{Adsorption (\%)} = ((C_0 - C_t)/C_0) * 100 \quad (1)$$

Where,  $C_0$  and  $C_t$  are the initial concentration of  $\text{Cu}^{2+}$ ,  $\text{Fe}^{2+}$  and  $\text{Mn}^{2+}$  ions (see Table 1) and concentration at time  $t$ , respectively. So, in Fig. 6 the residual concentration of  $\text{Cu}^{2+}$ ,  $\text{Fe}^{2+}$  and  $\text{Mn}^{2+}$  ions in mine drainage solution for known mass of modified perlite nanoparticles were showed.

The effect of temperature on  $\text{Cu}^{2+}$ ,  $\text{Fe}^{2+}$  and  $\text{Mn}^{2+}$  ions removal from aqueous solution was considered for three temperatures 25, 45 and  $65^\circ\text{C}$ . The results of temperature changes were showed in Fig. 7. With observing Fig. 7, it is obvious that by increasing in temperature the removal of heavy metal pollutants increased.

The amount of adsorption at equilibrium  $q_e$  (mg/g) was calculated according to the expression:

$$q_e (\text{mg / gr}) = \frac{(C_0 - C_e)V}{m} \quad (2)$$

where,  $C_0$  and  $C_e$  are the initial and equilibrium concentrations (mg/L),  $V$  the volume of solution (L),  $m$  the weight of modified perlite nanoparticles adsorbents (gr). Different masses of adsorbent,  $m$ , were dosed to 25 ml of the system investigated and then the system was agitated until the equilibrium was reached. The sorption time needed to reach the equilibrium increased when  $m$  was increased. The dependences of equilibrium amounts of sorbed  $\text{Cu}^{2+}$ ,  $\text{Fe}^{2+}$  and  $\text{Mn}^{2+}$  ions on the adsorption time for different masses of adsorbent are shown in Fig. 8.

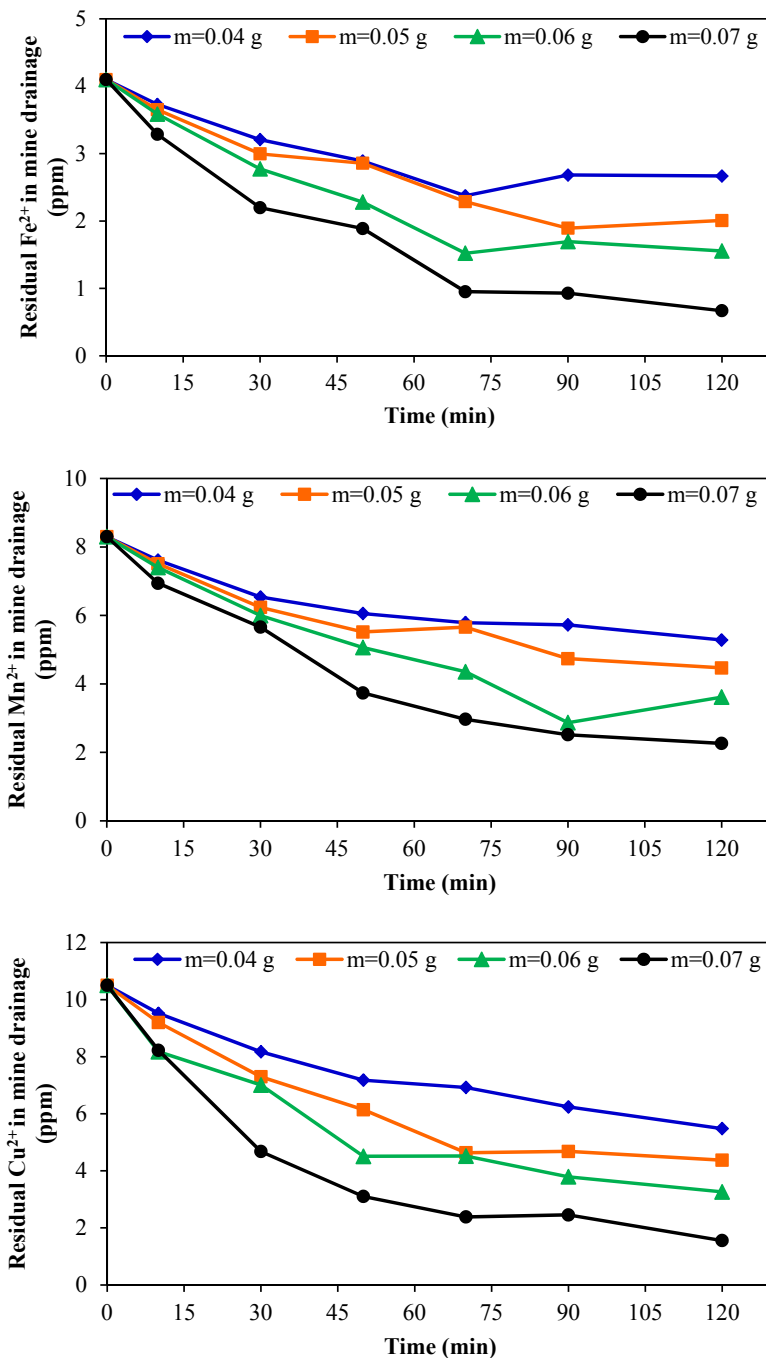


Fig. 6. Effect of adsorbent dose on the adsorption of Fe<sup>2+</sup>, Mn<sup>2+</sup> and Cu<sup>2+</sup> heavy metals by modified perlite nanoparticles for pH = 5.1, C<sub>0-Cu<sup>2+</sup></sub> = 10.5 ppm, C<sub>0-Fe<sup>2+</sup></sub> = 4.1 ppm, C<sub>0-Mn<sup>2+</sup></sub> = 8.3 ppm, C<sub>0-other ions</sub> = 1.24 ppm, V = 25 ml and Temperature = 25°C and m = mass g



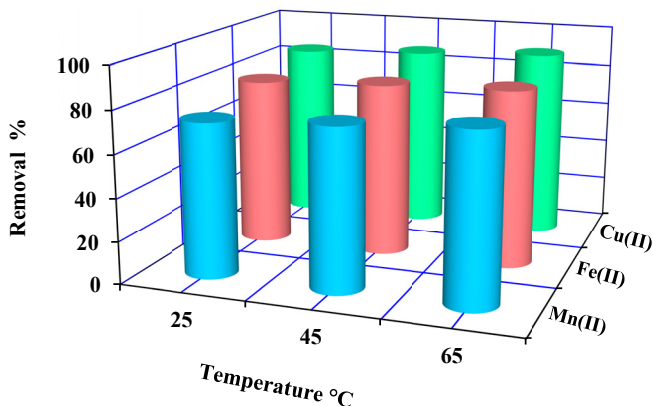


Fig. 7. Effect of temperature on the adsorption of heavy metal pollutants by modified perlite nanoparticles from acid mine drainage for  $pH = 5.1$ , adsorbent dose = 0.07 gr and Volume = 25 ml

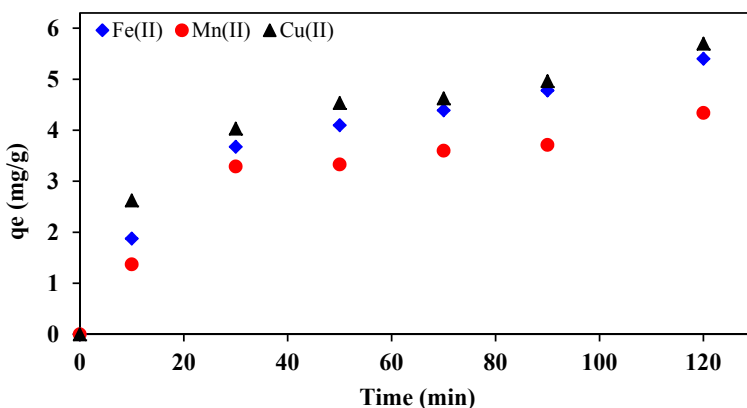


Fig. 8. The dependences of equilibrium amounts of sorbed  $Cu^{2+}$ ,  $Fe^{2+}$  and  $Mn^{2+}$  ions on the adsorption time for different adsorbents masses, m

## 2.2. Isotherms and kinetics of heavy metal pollutants adsorption from acid mine drainage

### 2.2.1. Sorption isotherm

Generally, adsorption isotherms provide vital information in optimizing the use of adsorbents. Descriptions on affinity between sorbates and sorbents, bond energy and adsorption capacity, to mention a few, can be extracted from isotherm equilibrium models applicable to adsorption processes (Ijagbemi et al., 2009). The equilibrium data were analyzed in accordance with the Langmuir, Freundlich and Temkin isotherm models. All of the models are listed in Table 4.

TABLE 4

Isotherm models, their linear forms and respective coefficients (Zheng et al., 2009)

Isotherm model	Equation	Linear form	Plot
Langmuir	$q_e = \frac{q_m K_L C_e}{1 + K_L C_e}$	$\frac{C_e}{q_e} = \frac{1}{K_L q_m} + \frac{1}{q_m} C_e$	$\frac{C_e}{q_e}$ VS. $C_e$
Freundlich	$q_e = K_F C_e^{1/n}$	$\ln(q_e) = \ln K_F + \frac{1}{n} \ln C_e$	$\ln q_e$ VS. $\ln C_e$
Temkin	$q_e = \frac{RT}{b} \ln(K_T C_e)$	$q_e = \frac{RT}{b} \ln K_T + \frac{RT}{b} \ln C_e$	$q_e$ VS. $\ln C_e$

where, in Table 4, in Langmuir isotherm  $q_m$  is a constant related to the area occupied by a monolayer of adsorbate, reflecting the maximum adsorption capacity (mg/g),  $C_e$  is the equilibrium concentration of solution (mg/l),  $K_L$  is a direct measure of the intensity of adsorption (l/mg) and  $q_e$  is the amount adsorbed at equilibrium (mg/g). In Freundlich isotherm,  $K_F$  ((mg/g)(l/mg)<sup>1/n</sup>) and  $n$  (dimensionless) are constants incorporating all factors affecting the adsorption process such as adsorption capacity and intensity, respectively. In Tempkin isotherm  $R$  is the gas constant (8.314 J/mol K),  $T$  is the absolute temperature (K) and  $b$  is the Temkin constant related to heat of sorption (J/mol).

Isotherm parameters for various two parameters adsorption isotherms for the adsorption of Cu<sup>2+</sup>, Fe<sup>2+</sup> and Mn<sup>2+</sup> ions onto modified perlite nanoparticles adsorbents at 25.0°C were showed in Table 5. It was found that the Langmuir isotherm showed better correlation with the experimental data than other isotherms.

TABLE 5

Langmuir, Freundlich and Tempkin isotherm constants for the adsorption of Cu<sup>2+</sup>, Fe<sup>2+</sup> and Mn<sup>2+</sup> ions onto modified perlite nanoparticles adsorbent

Isotherm model	Parameters	Three ions
		Cu <sup>2+</sup> + Fe <sup>2+</sup> + Mn <sup>2+</sup>
Langmuir	$q_m$ (mg g <sup>-1</sup> )	5.13
	$K_L$	0.63
	$R^2$	<b>0.986</b>
Freundlich	$K_F$	9.17
	$n$	5.85
	$R^2$	0.819
Tempkin	$B1$	1.06
	$K_T$	3423.05
	$R^2$	0.841

Square of correlation coefficient of the fit to experimental data ( $R^2$ ) showed that the uptake of Cu<sup>2+</sup> + Fe<sup>2+</sup> + Mn<sup>2+</sup> ions onto modified perlite nanoparticles adsorbent could be described by the Langmuir model.

### 2.2.2. Sorption kinetic

The kinetic of the adsorption process was analyzed using the pseudo-first-order and pseudo-second-order equations and intra-particle diffusion model to model the kinetics of  $\text{Cu}^{2+} + \text{Fe}^{2+} + \text{Mn}^{2+}$  ions adsorption onto modified perlite nanoparticles adsorbent. Three kinetic models are listed in Table 6.

TABLE 6

Kinetic models, their linear forms and respective coefficients (Najafi et al., 2011)

Kinetic model	Equation	Linear form	Plot
Pseudo first-order	$\frac{dq_t}{dt} = k_1(q_e - q_t)$	$\ln(q_e - q_t) = \ln q_e - k_1 t$	$\ln(q_e - q_t)$ VS. $t$
Pseudo-second-order	$\frac{dq_t}{dt} = k_2(q_e - q_t)^2$	$\frac{t}{q_t} = \frac{1}{k_2 q_e^2} + \frac{1}{q_e} t$	$\frac{t}{q_t}$ VS. $t$
intra-particle diffusion model	$q_t = \frac{K_i}{m} t^{(0.5)}$	$q_t = \frac{K_i}{m} t^{(0.5)}$	$q_t$ VS. $t^{(0.5)}$

Where in Table 6  $q_e$  and  $q_t$  are the amounts of metal ions adsorbed on the adsorbent ( $\text{mg g}^{-1}$ ) at equilibrium and at time  $t$ , respectively,  $k_1$  is the rate constant of the first-order adsorption in  $\text{min}^{-1}$  and  $k_2$  is the rate constant of second-order adsorption in  $(\text{g mg}^{-1} \text{min}^{-1})$ , also for intra-particle diffusion model  $m$  is the mass of sorbent (g),  $q_t$  the amount of solute adsorbed at time  $t$  ( $\text{mg/g}$ ) and  $K_i$  is the initial rate of intra-particle diffusion ( $\text{mg/l s}^{-1/2}$ ). The values of parameters obtained by different kinetic and intra-particle diffusion model for the adsorption of  $\text{Cu}^{2+} + \text{Fe}^{2+} + \text{Mn}^{2+}$  ions adsorption onto modified perlite nanoparticles adsorbent were showed in Table 7.

TABLE 7

The values of parameters obtained by different kinetic models for the adsorption of  $\text{Cu}^{2+}$ ,  $\text{Fe}^{2+}$  and  $\text{Mn}^{2+}$  ions adsorption onto modified perlite nanoparticles adsorbent

Kinetic model	Parameters	Ions
		$\text{Cu}^{2+} + \text{Fe}^{2+} + \text{Mn}^{2+}$
Pseudo-first order	$K_1$ ( $\text{min}^{-1}$ )	0.03
	$q_e$ ( $\text{mg g}^{-1}$ )	0.3
	$R^2$	0.792
Pseudo-second order	$K_2$ ( $\text{g mg}^{-1} \text{min}^{-1}$ )	0.05
	$q_e$ ( $\text{mg g}^{-1}$ )	8.27
	$R^2$	0.969
intra-particle diffusion model	$K_i$	0.688
	$R^2$	0.882

The correlation coefficient for the pseudo-second-order kinetic model for modified perlite nanoparticles is 0.969. The high correlation coefficients and the agreement of calculated and

experimental  $q_e$  both demonstrated that the adsorption kinetics of  $\text{Cu}^{2+}$ ,  $\text{Fe}^{2+}$  and  $\text{Mn}^{2+}$  ions adsorption onto modified perlite nanoparticles adsorbent followed the pseudo-second-order kinetic model. Therefore, the rate-limiting step may be chemical sorption or chemisorptions through sharing or exchange of electrons between sorbent and adsorbate.

### 2.2.3. Thermodynamic parameters

The amounts of  $\text{Cu}^{2+}$ ,  $\text{Fe}^{2+}$  and  $\text{Mn}^{2+}$  ions uptakes at 298.15, 318.15 and 338.15 K temperatures were calculated to obtain the thermodynamic parameters which were evaluated using the Van't Hoff equation (Urano and Tachikawa, 1991):

$$\log K_d = \frac{\Delta S^\circ}{2.303 R} - \frac{\Delta H^\circ}{2.303 RT} \quad (3)$$

The values of  $\log K_d$  were defined as follow:

$$K_d = \frac{a}{1-a} \quad (4)$$

where,  $\Delta S^\circ$  and  $\Delta H^\circ$  are entropy (kJ/mol K) and enthalpy (kJ/mol) change of adsorption, respectively,  $R$  is universal gas constant (8.314 J/mol K), and  $T$  is the absolute temperature (K),  $K_d$  is the equilibrium constant and  $a$  is uptake percentage of adsorbate at equilibrium. The values of  $\Delta H^\circ$  and  $\Delta S^\circ$  were calculated from the slope and intercept of linear regression of  $\ln(K_d)$  vs.  $(1/T)$ . Values of  $\Delta G^\circ$  were estimated by:

$$\Delta G = -RT \ln K_d \quad (5)$$

Calculated thermodynamic parameters such as  $\Delta H^\circ$ ,  $\Delta S^\circ$  and  $\Delta G^\circ$  are given in Table 8.

TABLE 8

Values of thermodynamic parameters for the adsorption of  $\text{Cu}^{2+} + \text{Fe}^{2+} + \text{Mn}^{2+}$  ions on modified perlite nanoparticles adsorbents

Ions	$\Delta H$ (kJ mol <sup>-1</sup> )	$\Delta S$ (J mol <sup>-1</sup> K <sup>-1</sup> )	$\Delta G$ (kJ mol <sup>-1</sup> )		
			298.15°K	318.15°K	338.15°K
$\text{Cu}^{2+} + \text{Fe}^{2+} + \text{Mn}^{2+}$	0.108089	0.033258	-9.80778	-10.4729	-11.1381

The negative values of  $\Delta G^\circ$  indicate that the sorption of  $\text{Cu}^{2+} + \text{Fe}^{2+} + \text{Mn}^{2+}$  ions from acid mine drainage onto modified perlite nanoparticles adsorbent were spontaneous processes. Change in enthalpy ( $\Delta H^\circ$ ) values is positive, showing that the sorption of  $\text{Cu}^{2+}$ ,  $\text{Fe}^{2+}$  and  $\text{Mn}^{2+}$  ions are endothermic in nature. All ions uptake increased with the increasing of temperature (see Fig. 7). The sorption of all ions also require a diffusion process, which is an endothermic process; i.e., the rise of temperatures favors  $\text{Cu}^{2+}$ ,  $\text{Fe}^{2+}$  and  $\text{Mn}^{2+}$  ions transport within the particles of modified perlite nanoparticles. In another aspect, the exchanges of the metal ions with  $\text{H}^+$  need first the bond breaking of OH, which is one of the possible existing forms of proton in modified perlite nanoparticles. The bond breaking is also an endothermic process. The  $\Delta H^\circ$  of  $\text{Cu}^{2+}$ ,  $\text{Fe}^{2+}$  and  $\text{Mn}^{2+}$  ions uptake by modified perlite nanoparticles is as  $\text{Cu}^{2+}$ ,  $\text{Fe}^{2+}$  and  $\text{Mn}^{2+}$  ions, that implying, temperature has a more important influence on  $\text{Mn}^{2+}$ ,  $\text{Fe}^{2+}$  and  $\text{Cu}^{2+}$  uptake, respectively. The

positive low values of  $\Delta S^\circ$  indicate low randomness at the solid/solution interface during the uptake of  $\text{Cu}^{2+}$ ,  $\text{Fe}^{2+}$  and  $\text{Mn}^{2+}$  ions onto modified perlite nanoparticles adsorbent.

Since,  $\Delta H > 0$  and  $\Delta S > 0$ , thus enthalpy and entropy are unfavorable and favorable agent, respectively, scilicet entropy cause to the adsorption processes was done to more adsorption and enthalpy cause to the adsorption processes was done to less adsorption. So, these adsorption processes are bilateral and can be done spontaneous. Also, at the reactions that enthalpy and entropy is inversely, the temperature is determinant agent, hence at the high temperatures the entropy is predominant agent and at the low temperatures the enthalpy is effective agent.

### 2.3. Continuous mode adsorption studies

After characterization, preparation and batch mode adsorption studies, the adsorbent was packed inside a glass column, where it was used for the adsorption/removal of  $\text{Cu}^{2+}$ ,  $\text{Fe}^{2+}$  and  $\text{Mn}^{2+}$  ions from Sreghshmeah acid mine drainage. A schematic view of glass column was showed in Fig. 9.

The length and diameter of glass column are 20 cm and 2 cm, respectively. A known amount of nanoadsorbent was packed inside a glass column and  $\text{Cu}^{2+}$ ,  $\text{Fe}^{2+}$  and  $\text{Mn}^{2+}$  ions solution were allowed to flow inside the column with a certain flow rate. The metal ions concentration was determined before and after the treatment using atomic absorption spectroscopy PG-990 model.

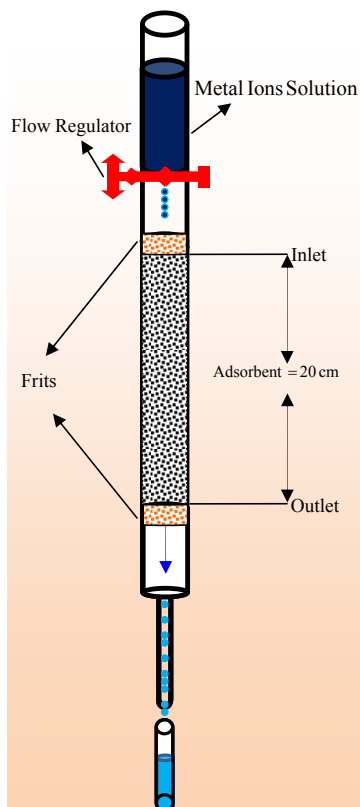


Fig. 9. Modified perlite nanoparticles adsorbent packed inside a glass column

So, the column of adsorbent were tested for all ions and obtaining the breakthrough curves. The breakthrough curves that obtained for  $\text{Cu}^{2+} + \text{Fe}^{2+} + \text{Mn}^{2+}$  ions adsorption by modified perlite nanoparticles adsorbent was showed in Fig. 10.

In the breakthrough curve if  $C_{inlet}$  (ion concentration at inlet or initial concentration) =  $C_{outlet}$  (ion concentration at outlet), therefore the saturation of adsorbent at column is occurs. The saturation time that occurs for ions adsorption onto modified perlite nanoparticles adsorbent for 1, 3 and 5 ml/min are 180, 240 and 315 min, respectively.

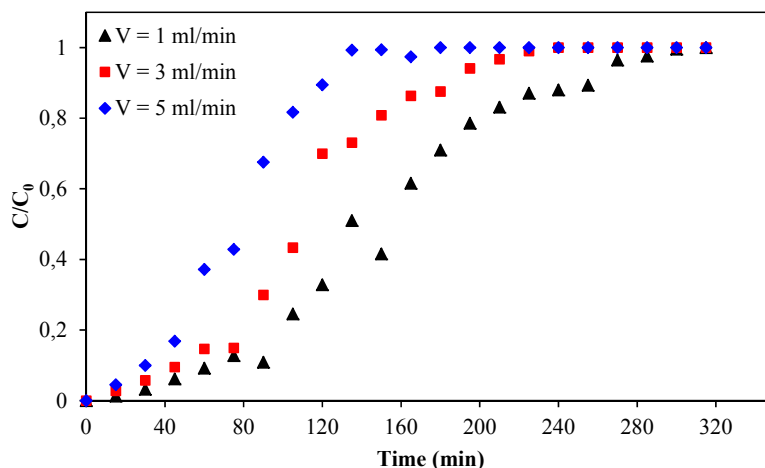


Fig. 10. The breakthrough curves of  $\text{Cu}^{2+} + \text{Fe}^{2+} + \text{Mn}^{2+}$  ions adsorption by modified perlite nanoparticles adsorbent

### 3. Conclusions

The surface properties and potential use of modified perlite nanoparticles as an adsorbent for iron (II), manganese (II) and copper (II) from Sarcheshmeh copper acid mine drainage was studied. Thus modified perlite nanoparticles that were prepared from internal resource (Zanjan mine, North West of Iran) firstly were modified and then characterized by XRD, XRF, SEM, TEM, FT-IR and BET analysis. XRD and XRF show that the main component is  $\text{SiO}_2$  (Nearly 60%). The FT-IR shows the positive effect of OH function in  $\text{SiO}_2$ , also in Fig. 6 the FT-IR spectra of modified perlite nanoparticles before and after Fe(II), Mn(II) and Cu(II) ions adsorption processes from acid drainage it is obvious the band  $B_5$  was OH weakened after Fe(II), Mn(II) and Cu(II) ions adsorption processes than before adsorption that due to OH function saturating by Fe(II), Mn(II) and Cu(II) ions. The BET analysis shows specific surface area  $89.7 \text{ m}^2/\text{gr}$  and  $3.5 \text{ m}^2/\text{gr}$  for modified perlite nanoparticles and raw perlite, respectively. In batch mode after the consideration of adsorbent dosage, the results of isotherm and kinetic studies show that the Langmuir isotherm and pseudo-second order kinetic have a good correlation with adsorption processes. Also, the maximum adsorption value for modified perlite nanoparticles is  $5.13 \text{ (mg/g)}$ . Calculations of thermodynamic parameters show that the negative  $\Delta G^\circ$  values at three different temperatures

suggest that the sorption of all metal ions from acid mine drainage were spontaneous. Change in enthalpy ( $\Delta H^\circ$ ) for all ions show the endothermic process, as ion uptake increased with increase in temperature. Values of  $\Delta S^\circ$  indicate low randomness at the solid/solution interface during the uptake of both all ions by adsorbents. In the long run, the modified perlite nanoparticles was packed inside a glass column and used for the removal of four ions from aqueous solution in several flow rates and obtaining the breakthrough curves. The saturation time that occurs for ions adsorption onto modified perlite nanoparticles adsorbent for 1, 3 and 5 ml/min are 180, 240 and 315 min, respectively. All results show that the ions affinity to adsorption onto adsorbents is as: Cu (II) > Fe (II) > Mn (II). The high selectivity in the bonding of iron (II), manganese (II) and copper (II) suggests modified perlite nanoparticles may be useful for removal of these toxic heavy metal ions and probably other heavy metal ions from other mining wastewaters. This ability can be explored in treatment technologies since perlite are cheap, abundant, and locally available resource.

### Acknowledgment

The authors appreciate the support of Shahrood University and Technology and Institute for Color Science and Technology towards the research paper.

### Reference

- Badii Kh., Doulati Ardejani F., Yousefi Limaee N., 2008. *A numerical finite element model for the removal of direct dyes from aqueous solution by soy meal hull: optimization and sensitivity analysis*. First Conference and Workshop on Mathematical Chemistry, Tarbiat Modares University, Tehran, Iran, 57-64.
- Caliskan N., Kul A.R., Alkan S., Sogut E.G., Alacabey I., 2011. *Adsorption of Zinc(II) on diatomite and manganese-oxide-modified diatomite: A kinetic and equilibrium study*. Journal of Hazardous Materials, 193, 27-36.
- Chiban M., Soudani A., Sinan F., Persin M., 2011. *Single, binary and multi-component adsorption of some anions and heavy metals on environmentally friendly Carpobrotus edulis plant*. Colloids and Surfaces B, 82, 267-276.
- Danil de Namor A.F., El Gamouz A., Frangie S., Martinez V., Valiente L., Webb O.A., 2012. *Turning the volume down on heavy metals using tuned diatomite. A review of diatomite and modified diatomite for the extraction of heavy metals from water*. Journal of Hazardous Materials, 241-242, 14-31.
- Doulati Ardejani F., Badii Kh., Yousefi Limaee N., S Shafaei.Z., Mirhabibi A.R., 2008. *Adsorption of Direct Red 80 dye from aqueous solution on to almond shell Effect of pH, initial concentration and shell type*. Journal of Hazardous Materials, 151: 2-3, 730-737.
- Ediz N., Bentli I., Tatar I., 2010. *Improvement in filtration characteristics of diatomite by calcination*. International Journal of Mineral Processing, 94, 129-134.
- Egashira R., Tanabe S., Habaki H., 2012. *Adsorption of heavy metals in mine wastewater by Mongolian natural zeolite*. Procedia Engineering, 42, 49-57.
- Fowler C.E., Buchber C., Lebeau B., Patarin J., Delacote C., Walcarius A., 2007. *An aqueous route to organically functionalized silica diatom skeletons*. Applied Surface Science, 253, 5485-5493.
- Ghassabzadeh H., Mohadespour A., Torab-Mostaedi M., Zaheri P., Maragheh M.G., Taheri H., 2010. *Adsorption of Ag, Cu and Hg from aqueous solutions using expanded perlite*. Journal of Hazardous Materials, 177, 950-955.
- Hong L., Minoru T., 1994. *Mechanical strength increase of abraded silica glass by high pressure water vapor treatment*. Journal of Non-Crystalline Solids, 168, 287-292.
- Ijagbemi Ch.O., Baek M.H., Kim D.S., 2009. *Montmorillonite surface properties and sorption characteristics for heavy metal removal from aqueous solutions*. Journal of Hazardous Materials, 166, 538-546.
- Jing Q., Fang L., Liu H., Liu P., 2011. *Preparation of surface-vitrified micron sphere using perlite from Xinyang*. China Applied Clay Science, 53, 745-748.
- Karami H., 2013. *Heavy metal removal from water by magnetite nanorods*. Chemical Engineering Journal, 219, 209-216.

- Kyzas G.Z., Kostoglou M., Lazaridis N.K., Bikiaris D.N., 2013. *N-(2-Carboxybenzyl) grafted chitosan as adsorptive agent for simultaneous removal of positively and negatively charged toxic metal ions*. Journal of Hazardous Materials, 244-245, 29-38.
- Li X., Liu L., Wang Y., Luo G., Chen Xi., Yang X., Hall M.H.P., Guo R., Wang H., Cui J., He X., 2012. *Heavy metal contamination of urban soil in an old industrial city (Shenyang) in Northeast China*. Geoderma, 192, 50-58.
- Lopes G., Guilherme L.R.G., Costa E.T.S., Curi N., Penha H.G.V., 2012. *Increasing arsenic sorption on red mud by phosphogypsum addition*. Journal of Hazardous Materials. In Press.
- Lugo-Lugo V., Barrera-Díaz C., Ureña-Núñez F., Bilyeu B.I., 2012. *Linares-Hernández, Biosorption of Cr(III) and Fe(III) in single and binary systems onto pretreated orange peel*. Journal of Environmental Management, 112, 120-127.
- Martins A., Mata T.M., Gallios G.P., Václavíková M., Stefusova K., 2010. *Modeling and simulation of heavy metals removal from drinking water by magnetic zeolite, Water Treatment Technologies for the Removal of High-Toxicity Pollutants*. Project No. APVT-51-017104, 24 p.
- Miretzky P., Saralegui A., Cirelli A.F., 2006. *Simultaneous heavy metal removal mechanism by dead macrophytes*. Chemosphere, 62, 247-254.
- Muller B.R., 2010. *Effect of particle size and surface area on the adsorption of albumin-bonded bilirubin on activated carbon*. Carbon, 48, 3607-3615.
- Najafi M., Yousefi Y., Rafati A.A., 2011. *Synthesis, characterization and adsorption studies of several heavy metal ions on amino-functionalized silica nano hollow sphere and silica gel*. Separation and Purification Technology, 85, 193-205.
- Niu Ch., Wu W., Zhu W., Li Sh., Wang J., 2007. *Adsorption of heavy metal ions from aqueous solution by crosslinked carboxymethyl konjac glucomannan*. Journal of Hazardous Materials, 141, 209-214.
- Pehlivan E., Altun T., 2008. *Biosorption of chromium(VI) ion from aqueous solutions using walnut, hazelnut and almond shell*. Journal of Hazardous Materials, 155: 1-2, 378-384.
- Rouliá M., Chassapis K., Kapoutsis J.A., Kamitsos E.I., Savvidis T., 2006. *Influence of thermal treatment on the water release and glassy structure of perlite*. Journal of Material Science, 41, 5870-5881.
- Schiewer S., Volesky B., 1995. *Modeling of the proton-metal ion exchange in biosorption*. Environmental Science & Technology, 29, 3029-3058.
- Seifpanahi Shabani K., Doulati Aredejani F., Singh R.N., Marandi R., Soleimanyfar H., 2011. *Numerical Modeling of Cu<sup>2+</sup> and Mn<sup>2+</sup> Ions Biosorption by Aspergillus Niger Fungal Biomass in A Continuous Reactor*. Archive of Mining Sciences, 56: 3, 461-476.
- Sheikhhosseini H., Shirvani M., Shariatmadari H., 2013. *Competitive sorption of nickel, cadmium, zinc and copper on palygorskite and sepiolite silicate clay minerals*. Geoderma, 192, 249-253.
- Sodeyama K., Sakka Y., Kamino Y., Seki H., 1999. *Preparation of fine expanded perlite*. Journal of Material Science, 34, 2461-2468.
- Song J., Oh H., Kong H., Jang J., 2011. *Polyrhodanine modified anodic aluminum oxide membrane for heavy metal ions removal*. Journal of Hazardous Materials, 187: 1-3, 311-317.
- Thanh D.N., Singh M., Ulbrich P., Strnadova N., Štěpánek F., 2011. *Perlite incorporating  $\gamma$ -Fe<sub>2</sub>O<sub>3</sub> and  $\alpha$ -MnO<sub>2</sub> nanomaterials: Preparation and evaluation of a new adsorbent for As(V) removal*. Separation and Purification Technology, 82, 93-101.
- U.S. Environmental Protection Agency, 2011. *Technical Document: Acid Mine Drainage Prediction*. EPA 820-R-11-002, Office of Water U.S. Environmental Protection Agency Washington, DC.
- Urano K., Tachikawa H., 1991. *Process-development for removal and recovery of phosphorus from waste-water by a new adsorbent 2: adsorption rates and breakthrough curves*. Industrial & Engineering Chemistry Research, 30, 1897-1899.
- Varuzhanyan Av.A., Varuzhanyan Ar.A., Varuzhanyan H.A., 2006. *A mechanism of perlite expansion*. Inorganic Materials, 42, 1039-1045.
- Yuan P., Liu D., Fan M., Yang D., Zhu R., Ge F., Zhu J.X., He H., 2010. *Removal of hexavalent chromium [Cr(VI)] from aqueous solutions by the diatomite-supported/unsupported magnetite nanoparticles*. Journal of Hazardous Materials, 173, 614-621.
- Yuan P., Wu D.Q., He H.P., Lin Z.Y., 2004. *The hydroxyl species and acid sites on diatomite surface: a combined IR and Raman study*. Applied Surface Science, 227, 30-39.
- Zheng H., Liu D., Zheng Y., Liang S., Liu Z., 2009. *Sorption isotherm and kinetic modeling of aniline on Cr-bentonite*. Journal of Hazardous Materials, 167, 141-147.